LAWRENCE
LIVERMORE
NATIONAL
LABORATORY

LLNL-CONF-544133

Rupture Model for a Characterized Intraslab Earthquake

A. Pitarka, S. Matsuzaki, T. Watanabe, N. Collins, R. Graves , P. Somerville

April 2, 2012

15th World Conference on Earthquake Engineering
Lisbon, Portugal
September 24, 2012 through September 28, 2012

Disclaimer

Rupture Model for a Characterized Intraslab Earthquake

Arben Pitarka
Lawrence Livermore National Laboratory, Livermore, California. U.S.A.

Shin'ichi Matsuzaki
Shikoku Electric Power Company, Japan

Takahide Watanabe
Ohsaki Research Institute, Shimizu Corporation, Japan

Nancy Collins
URS Corporation, Los Angeles, California, U.S.A.

Robert Graves
USGS, Pasadena, California, U.S.A.

Paul Somerville
URS Corporation, Los Angeles, California, U.S.A.

SUMMARY
In this study we analyze the performance of the Irikura and Miyake (2006) procedure for characterizing kinematic rupture models for intraslab earthquakes. The characterization approach provides simple rules for specifying the size, location, rise time and strength of slip asperities. The procedure was tested against strong ground motions recorded during the Mw6.7, 2001 Geiyo, Japan earthquake. The earthquake source used in the ground motion simulations is specified by the kinematic description of the fault rupture that incorporates spatial heterogeneity in slip and rise time. In the proposed characterized model the asperity locations and rupture initiation point were the only parameters that were initially constrained by the available rupture models of the target earthquake. The quality of the characterized rupture model was assessed by comparing recorded and synthetic ground motion time histories calculated with a standard broadband (0.1-10 Hz) ground motion simulation technique. Our analyses show that the characterized rupture model performs well in reproducing the recorded ground motion, in spite of the simplified representation of the fault geometry and kinematic rupture complexity. The analyses of ground motion sensitivity to relative location of asperities, and their stress drop contrast show that the overall ground motion goodness-of-fit remains relatively unchanged at short periods, but slightly degrades at periods longer than 1 sec. This result suggests that the high frequency part of ground motions from intraslab earthquakes is relatively insensitive to details of the slip distribution and slip contrast.

Keywords: Strong Ground Motion, Broad Band Simulation Technique, Intraslab Earthquake

1. INTRODUCTION

In this study we present a kinematic rupture model of the 2001 Geiyo, Japan earthquake. The rupture model is parameterized based on Irikura and Miyake (2006) procedure. The quality of the proposed methodology for characterizing the rupture model of intraslab earthquakes was assessed by comparing recorded and synthetic ground motion calculated with a standard broadband (0.1-10 Hz) ground motion simulation technique (Graves and Pitarka, 2010). The 2001 Geiyo, earthquake (Mw=6.7) is an intraslab earthquake. It occurred on a normal fault in the Philippine Sea slab subducting beneath the southwestern part of Japan. Although of moderate magnitude this deep earthquake generated very strong ground motion in a large area above the hypocenter. Studies of its source process based on inversions of different types of data have provided important information about the rupture process and its effect on the recorded near-fault ground motion.

2. RUPTURE MODEL

The 2001 Geiyo earthquake was recorded by a dense network of strong motion stations. The stations we selected to use in this study are shown in Figure 1. The network provided high quality data that were essential in obtaining reliable kinematic and dynamic models of the earthquake rupture (Kakehi 2004; Sekiguchi and Iwata (2002); Yagi and Kikuchi, 2001; Miyatake et al.,2003; Asano et al., 2003). In our procedure the earthquake source is specified by the kinematic description of the fault model that incorporates spatial heterogeneity in slip and rise time and constant rupture velocity. We used the kinematic slip model of Yagi and Kikuchi (2001), shown in Figure 2a, to constrain the fault geometry and the size and relative location of the asperities in our characteristic rupture model. The fault is 24 km long and 10.5 km wide. The depth to top of the fault is 45.3 km. The strike is 180^o, dip is 55^o and the rake is -82^o (Miyatake et al., 2004). We use a seismic moment of 1.51×10^{19} N*m obtained from F-net, NIED, Japan.

2.1. Slip Parameterization

In our model the asperities (regions of large slip) are represented by two rectangular areas with larger stress drop. The fault geometry and asperity locations are depicted in Figure 2b. The total fault area S was estimated by fitting the source spectrum amplitude A', derived from the effective stress drop, to the source spectral amplitude estimated from near fault strong motion (Satoh, 2005). A' is calculated using the high frequency levels of amplitude spectra for the both asperities and background area Aa1, Aa2, and Ab, respectively:

$$A' = \sqrt{{A_{a1}}^2 + {A_{a1}}^2 + {A_b}^2}$$

where :

$$A_{a1} = 4\pi \times (S_{a1}/\pi)^{1/2} \times \Delta\sigma_{a1} \times \beta^2$$
$$A_{a2} = 4\pi \times (S_{a2}/\pi)^{1/2} \times \Delta\sigma_{a2} \times \beta^2$$
$$A_b = 4\pi \times (S_b/\pi)^{1/2} \times \Delta\sigma_b \times \beta^2$$

S_{a1}, S_{a2}, and S_b are the asperity and fault background areas, respectively. $\Delta\sigma_{a1}$, $\Delta\sigma_{a1}$, $\Delta\sigma_b$ are the stress drops in the asperities and fault background areas, respectively.
Based on the earthquake magnitude and following the Irikura and Miyake (2006) recipe, the ratio between the areas of the large asperity Sa1, and small asperity Sa2, was estimated to be 16:6. The slip in each asperity Da is twice the fault average slip D. The seismic moment for each asperity is:

$$M_{0a1} = M_{0a} \times \frac{{S_{a1}}^{1.5}}{{S_{a1}}^{1.5} + {S_{a2}}^{1.5}} \qquad M_{0a2} = M_{0a} - M_{0a1}$$

where M_{0a} is the total moment of asperity regions. M_{0a} is calculated as follows:

$$M_{0a} = \mu \times S_a \times D_a$$

The slip in both asperities and fault background region are:

$$D_{a1} = \frac{M_{0a}}{\mu \times S_{a1}} \qquad D_{a2} = \frac{M_{0a}}{\mu \times S_{a2}} \qquad D_b = \frac{M_{0b}}{\mu \times S_b}$$

where $S_b = S - S_a$ is the area of fault background region.

The effective stress drop $\Delta\sigma_e$ for each asperity is assumed to be the same, and is estimated as follows:

$$\Delta\sigma_e = \frac{S}{S_e}\Delta\sigma$$

where the average stress drop $\Delta\sigma$ is calculated using the circular crack approximation:

$$\Delta\sigma = \frac{7}{16}\times\frac{M_0}{R^3} = \frac{7}{16}\times\frac{M_0}{(S/\pi)^{1.5}}$$

The background effective stress drop $\Delta\sigma_b$ is estimated using the approach of Dan et al. (2002):

$$\Delta\sigma_b = (D_b/S_b^{1/2})\times(S_{a1}^{1/2}/D_{a1})\times\Delta\sigma_{a1}$$

By applying this procedure the fault area S was estimated to be 242 km^2. This yields a fault length of 24 km for a fault width of 10.5 km. The rupture initiation is centered in the larger asperity. Following Yagi and Kikuchi's mode, the depth to top of the fault is 45.3 km. The parameters of the characteristic model are shown in Table 1.

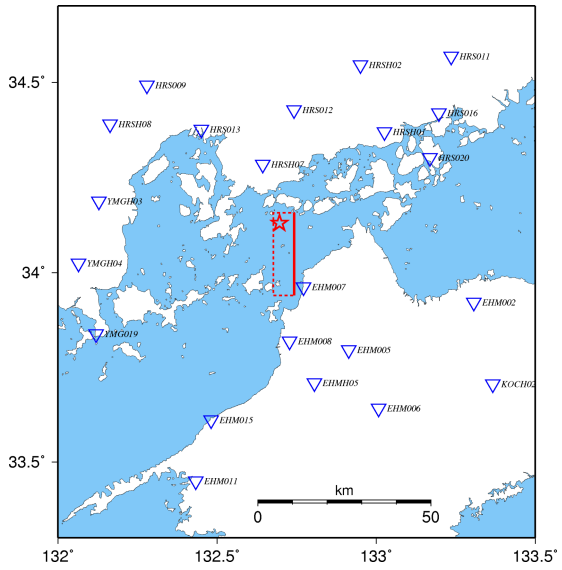

Figure 1. Map showing the fault projection of the 2001 Geiyo earthquake, and location of stations.

2.2. Slip Rate Function

The slip velocity function s(t) of the characteristic model is constructed using a functional form that was derived from dynamic rupture simulations (Nakamura and Miyatake, 2000). In our model the maximum slip velocity V_{max} is controlled by the seismic moment. The slip velocity functions corresponding to areas of background, large asperity, and small asperity of the characteristic earthquake rupture model are shown in Figure3.

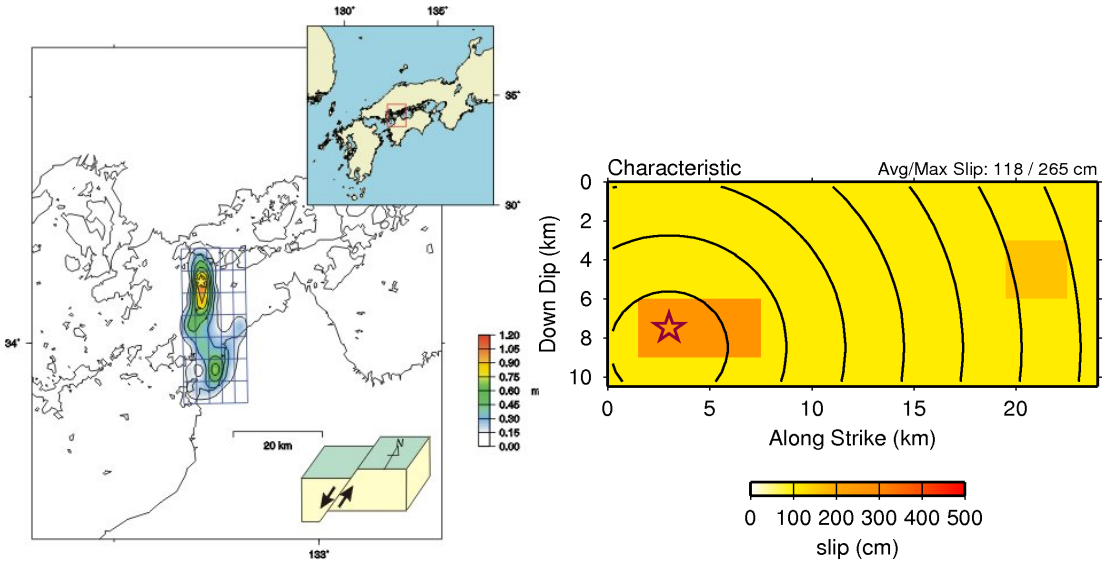

Figure 2. Left Panel: Slip model of the 2001 Geiyo earthquake proposed by Yagi and Kikuchi (2001). Right Panel: Slip model for a characteristic intraslab earthquake used in this study.

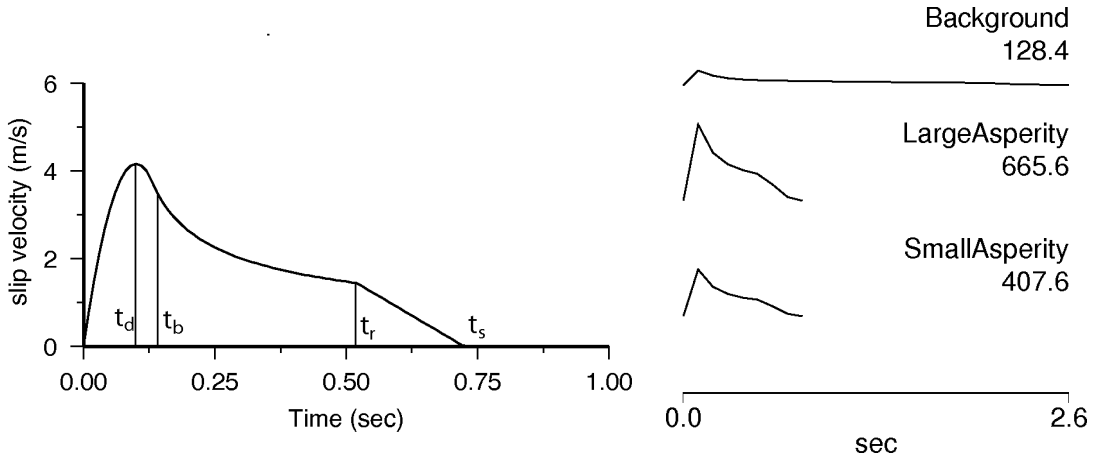

Figure 3. Left Panel: Slip rate function used in the deterministic simulation of rupture kinematics for the characteristic earthquake (Nakamura and Miyatake, 2000). Right Panel: Slip velocity functions for the background, large asperity, and small asperity areas of the characteristic earthquake rupture model. The peak slip velocity in cm/s is indicated on the right side of each slip velocity function.

Table 1. Earthquake Rupture Model

	Total	Asperities	Large Asperity	Small Asperity	Background Area
Mo	1.51E+19 N*m	Mo	2.46E+18 N*m	5.65E+17 N*m	1.21E+19N*m
Rigidity	5.28E+10 N/m^2	Area	17.6 km^2	6.6 km^2	217.8km^2
Vs	4.0 km/s	Dislocation	265 cm	162 cm	105 cm
Vr	2.88 km/s	Stress Drop	97.8 MPa	97.8 Mpa	11.0 MPa

3. GROUND MOTION SIMULATION

We simulated near-fault ground motion at selected stations that recorded the Geiyo earthquake using a broadband technique (Graves and Pitarka, 2010). Our simulation procedure follows a hybrid technique that computes the low frequency and high frequency ranges separately and then combines the two to produce a single time history (e.g.,Pitarka et al., 2000). The low frequency simulation methodology uses a deterministic representation of source and wave propagation effects and is based on the approach described by Hartzell and Heaton (1983). The basic calculation is carried out using either a 3D viscoelastic finite-difference algorithm (Graves 1996; Pitarka, 1999), which incorporates both complex source rupture as well as wave propagation effects within arbitrarily heterogeneous 3D geologic structure, or a wavenumber integration method using a 1D velocity model. The earthquake source is specified by the slip distribution, rupture velocity and rise time.

The high frequency (f > 1 Hz) simulation methodology computes the response assuming a random phase, an omega-squared source spectrum, and simplified Green's functions (e.g., Pitarka et al., 2000). The methodology follows from Boore (1983) with the extension to finite-faults given by Frankel (1995). The source is represented by subfaults that rupture with a moment proportional to the final slip given by the original source model. The subfault moment values are scaled uniformly so that the total moment matches that of the original source model. The subfault corner frequency (f_c) is defined by

$$f_c = s_z s_t \frac{v_r}{\pi d}$$

where v_r is the rupture speed, d is the subfault dimension, s_z scales the corner frequency with depth, and s_t relates the corner frequency to the rise time of the subfault source. For application to crustal earthquakes, we use a uniform value of $s_t = 1.6$. From the surface to a depth of 5 km, the depth scaling factor is set to a constant value, $s_z = 1.0$. This value increases linearly with depth to a value of $s_z = 1.4$ at 10 km. From 10 km depth to the Moho, s_z is constant at 1.4. This parameterization follows from the observation in crustal earthquakes that slip rate is relatively low for shallow ruptures and increases with rupture depth. For application to high stress-drop intraslab events such as the Geiyo earthquake, the factor s_z is increased by another 50% to a value of 2.1. The convolution operator of Frankel (1995) scales the subevent corner frequency to the corner frequency of the target event.

In this study, we use a 1D velocity model that roughly follows the average depth variations in the 3D structure. In our high frequency Green's functions we include both direct and Moho-reflected rays, which are attenuated by $1/R_p$, where R_p is the total path length traveled by the particular ray. For each ray we compute a radiation pattern coefficient by averaging over a range of slip mechanisms and take-off angles. Anelasticity is incorporated via a travel time weighted average of the Q values for each of the material layers and a generic rock site spectral decay operator, $\kappa = 0.05$. The synthetic seismograms are corrected for local site conditions using the technique proposed by Graves and Pitarka (2010) which requires V_s^{30} at the site of interest. Finally, the individual responses are combined into broadband response using a set of matched Butterworth filters. The filters are 4th-order and zero-phase with a low-pass corner at 1 Hz for the deterministic response and a high-pass corner at 1 Hz for the stochastic response.

3.1. 1D Velocity Models and Correction for Site Effects

The velocity model of the crust used in this study is shown in Table 2. It is based on the work by Kakehi (2004) except for the top four layers. For the high frequency simulations the top two layers are replaced by a series of thin layers in which the shear wave velocity gradually increases from 0.865 km/s at the free surface to 2.8 km/s at 200 m depth. For each of the 22 strong motion sites, site category and V_{s30} (travel-time averaged shear wave velocity to a depth of 30 m) values are obtained from the available shallow soil profile at the station site. The available soil and velocity profiles at the K-net recording sites only extend to a depth of 20 m. Based on this limited information, approximate V_{s30} values have been estimated for use in the simulation. Using the technique of Graves and Pitarka (2010), we then construct frequency-

dependent amplification functions that are applied to the results of the deterministic and stochastic simulations.

Table 2. 1D Velocity Model of the Crust

Thickness (km)	Vp (km/s)	Vs(km/s)	Density (g/cm^3)	Qp	Qs
0.01	5.3	2.6	3.0	100	50
0.19	5.5	2.7	3.0	100	50
1.8	5.7	2.8	3.0	380	190
14.0	6.1	3.5	3.0	460	230
24.0	6.7	3.87	2.8	800	400
2.0	6.6	3.82	2.8	800	400
4.0	6.7	3.87	2.9	800	400
	8.0	4.62	3.2	2400	1200

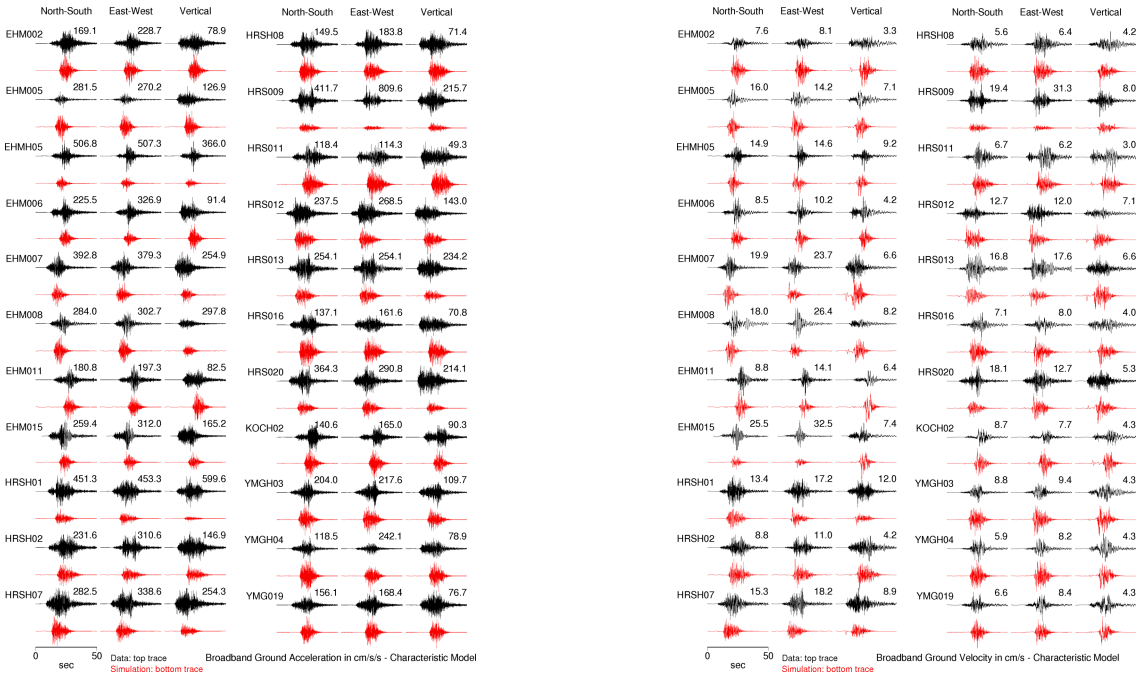

Figure 4. Comparison of three-component time histories of broadband acceleration (left panel) and velocity (right panel). Black traces indicate recorded wave forms and red traces indicate synthetic waveforms calculated for the characteristic earthquake. The station name is shown on the left side of each set of traces and the maximum amplitude for each component is shown above the trace.

3.2. Simulated Ground Motion Using the Characteristic Rupture Model

We analyzed the effectiveness of the procedure for characterizing the kinemtic rupture model by comparing the simulated and recorded ground motion data. Figure 4 compares the observed and simulated three-component ground velocities and accelerations at the 22 sites. These sites include near-fault locations. Figure 5 compares the observed and simulated acceleration response spectra for the sites. In general the agreement between the observed and simulated spectra is very good at all periods. We also compare the data and simulations using goodness-of-fit measures for 5% damped spectral acceleration

calculated from the broadband time histories. For an individual station, the residual $r(T_i)$ at each period T_i is given by $r(T_i) = \ln\left[sa_O(T_i) / sa_S(T_i)\right]$, where $sa_O(T_i)$ and $sa_S(T_i)$ are the observed and simulated spectral acceleration values, respectively. The model bias is obtained by averaging the residuals for all stations and both horizontal components at each period. A model bias of zero indicates the simulation, on average, matches the observed ground motion level. A negative model bias indicates over-prediction and a positive model bias indicates under-prediction of the observations. Figure 6 shows the model bias and standard error for the 22 simulations. The simulation result has a small bias in the period range 0.1 to 10 seconds, indicating that the simulation model adequately captures the main characteristics of the ground motion response.

4. MODEL SENSITIVITY ANALYSIS

As expected, due to planar fault assumption and simplifications, our model does not reproduce the waveform complexities especially at stations located on a direction perpendicular to the fault plane. The ground motion at these sites is sensitive to the asperity and rupture initiation locations.
In order to assess the sensitivity of the simulated ground motion to slip complexity we calculated ground motion from two additional characteristic rupture models, named Model A and Model B. These models were produced by altering the relative strength of the two asperities in the original characteristic rupture model. In Model A we increased the contrast of slip between the southern asperity and fault background by a factor of 3. In Model B we switched the asperity locations. The slip distributions for both models are shown in Figure 7. The goodness of fit between the simulated and recorded ground motion, shown in Figure 8, indicates that Model A generates somewhat larger ground motion in the E-W component, partly due to stronger directivity effects and higher slip in the southern asperity. Model B produces weaker motions than Model A, particularly at the longer periods and for the near fault sites. Model B produces weaker long period ground motions at near fault sites to the north of the rupture compared to those for both the characterized rupture model and Model A. Since Model B has much lower slip on the northern asperity than the other rupture models, this indicates the importance of large slip near the hypocenter for the Geiyo earthquake in order to satisfy the near fault ground motion observations.

5. CONCLUSIONS

The performance of the proposed kinematic rupture model and ground motion simulation methodology of Graves and Pitarka (2010) was tested against recorded ground motions from the 2001 Geiyo earthquake. The Irikura and Miyake (2006) methodology is designed to simulate ground motion for future earthquakes and allows for free selection of relative location of asperities and rupture initiation. In our model the asperity locations and rupture initiation point were the only parameters that were constrained by the available earthquake rupture models of the target earthquake. Our analyses show that the a rupture model developed using Irikura and Miyake (2006) methodology performs well in reproducing the recorded ground motions from the 2001 Geiyo earthquake, in spite of the simple representation of the fault geometry and kinematic rupture complexity.
The analyses of ground motion sensitivity to relative location of asperities and their stress drop contrast performed here, suggest that the overall ground motion goodness-of-fit remains the same at short periods, but slightly decreases different at periods longer than 1 sec. We suspect that, due to the depth of the intraslab source (40-50 km), the higher frequency ground motions are relatively insensitive to the details of the slip distribution and slip contrast. On the other hand the lower frequency motions are influenced by source radiation pattern, rupture directivity effects and slip distribution.
The broadband simulation methodology employed in this study has successfully been tested against crustal earthquakes (e.g. Pitarka et al., 2000; Graves and Pitarka, 2010). This is our first attempt to apply

it in association with the Irikura and Miyake (2006) recipe to simulate ground motions from intraslab earthquakes. The methodology produces favorable results when compared against the strong ground motions recorded during the 2001 Geiyo earthquake. The broadband simulation methodology presented here provides a general framework for synthesizing ground motion time histories for future intraslab scenario earthquakes.

6. ACKNOWLEDGEMENT

This work was performed under the auspices of the U.S. Department of Energy by Lawrence Livermore National Laboratory under Contract DE-AC52-07NA27344.

7. REFERENCES

Asano, K., T. Iwata, and K. Irikura (2003). Source characteristics of shallow intraslab earthquakes derived from strong motion simulations, *Earth Planets Space*, **55**, e5-e8.

Boore D. (1983). Stochastic simulation of high frequency ground motions based on seismological models of the radiated spectra, Bull. Seism. Soc. Am., 73, 1865-1894.

Dan, K., T. Sato, and K. Irikura (2002). Characterizing source model for strong motion prediction based on asperity model, *11-th Japan Earthquake Engineering Symposium*, pp 555-560. (in Japanese).

Frankel, A. (1995). Simulating strong motion of large earthquakes using recordings of small earthquakes: the Loma Prieta mainshock as a test case, *Bull. Seism. Soc. Am*. **85**, 1144-1160.

Graves, R., and A. Pitarka (2010). Broad band ground-motion using a hybrid approach. Bull. Seism. Soc. Am. 100, 2095–2123

Graves R. (1996). Simulating seismic wave propagation in 3D elastic media using staggered grid finite differences, *Bull. Seism. Soc. Am*., **86**, 1091-1106.

Hartzell S and T. Heaton (1983). Inversion of strong ground motion and teleseismic waveform data for the fault rupture history of the 1979 Imperial Valley, California earthquake, *Bull. Seism. Soc. Am.,* **73**, 1553-1583.

Irikura, K., and H. Miyake (2006). Recipe for predicting strong ground motions: the state of the arts and future prospects, *Proceedings of the 8-th U.S. National Conference on Earthquake Engineering, 2006, San Francisco, California, USA*, No.744.

Irikura K. (1978). Semi-empirical estimation of strong ground motions during large earthquakes. *Bull. Disast. Prev. Res. Inst., Kyoto Univ*., **33**, 63-104.

Kakehi (2004). Analysis of the 2001 Geiyo, Japan earthquake using high-density strong ground motion data: Detailed rupture process of a slab earthquake in a medium with a large velocity contrast, *J. Geophys. Res.*, **109**, B08306.

Miyatake , T., Y. Yagi, and T. Yasuda (2004). The dynamic rupture process of the 2001 Geiyo, Japan, earthquake. *Geophys. Res. Lett*., **31**, L1212.

Nakamura, H., and T. Miyatake (2000). An approximate expression of slip velocity time function for simulation of near-field strong motion, Zisin (J.Seism.Soc.Japan), 53, 1-9 (in Japanese)

Pitarka A. (1999). 3D elastic finite difference modeling of seismic wave propagation using staggered grid with non-uniform spacing, *Bull. Seism. Soc. Am*., **88,** 54-68.

Pitarka A., P. Somerville, Y. Fukushima, T. Uetake, and K. Irikura. (2000). Simulation of near-fault strong ground motion using hybrid Green's functions, *Bull. Seism. Soc. Am*., **90,** 566-586.

Satoh, T. (2005). Influence of fault mechanism, depth, and region on stress drop of small and moderate earthquakes in Japan, *Structural Eng./Earthquake Eng., Japan Society of Civil Engineers*, **23**, No1, 125-134.

Yagi, Y. and M. Kikuchi (2001). Kinematic rupture model of the 2001 Geiyo earthquake. http://iisee.kenken.go.jp/staff/yagi/Aki-nad

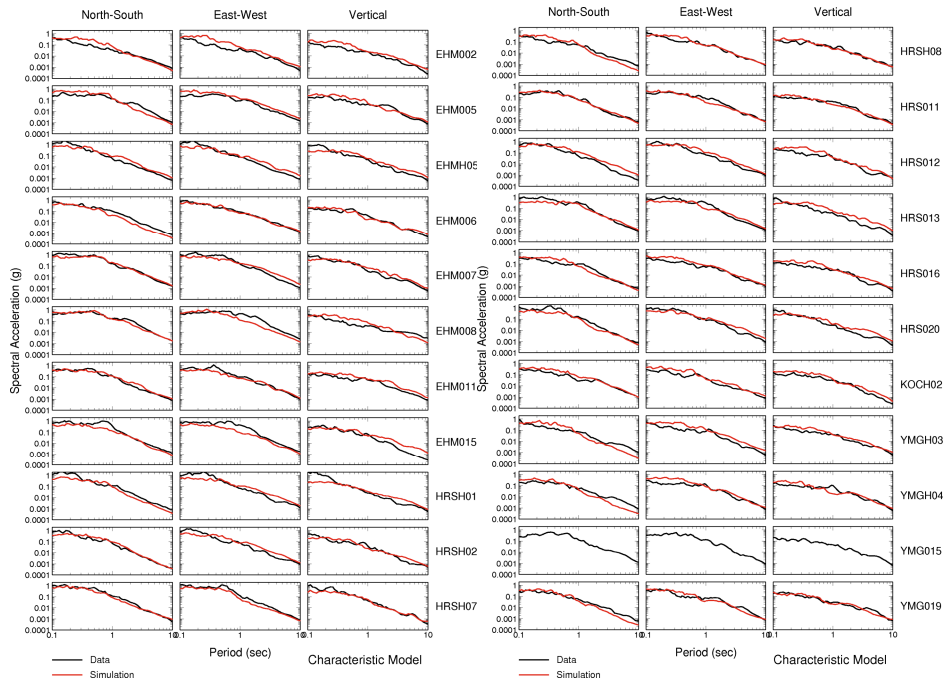

Figure 5. Comparison of recorded (black) and calculated (red) acceleration response spectra at 22 stations.

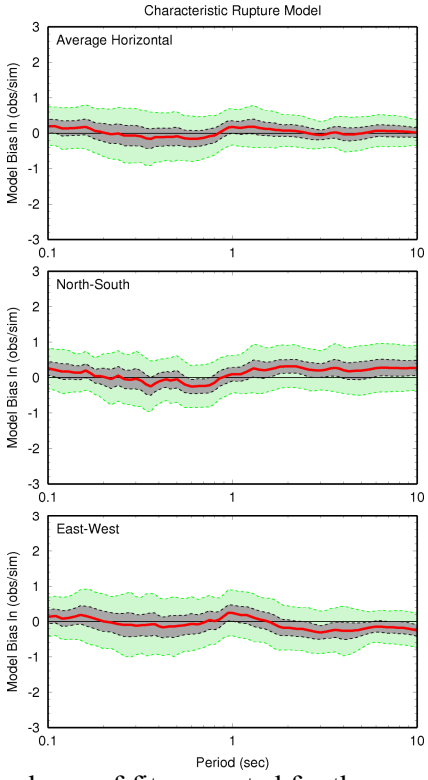

Figure 6. Spectral acceleration goodness-of-fit computed for the average of both horizontal components for the characteristic earthquake. Red line is mean model bias averaged over 22 sites. Gray shading denotes 90% confidence interval of the mean and green shading denotes interval of one standard deviation. Upper, middle and lower panels are average horizontal, NS and EW components, respectively.

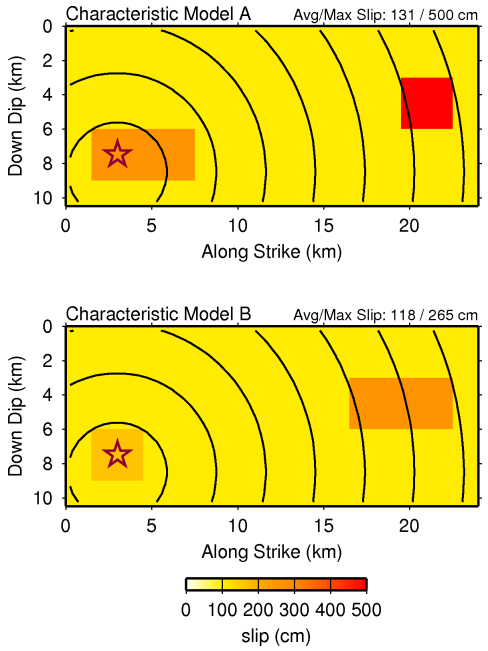

Figure 7. Slip models obtained based on modifications of the original slip model shown in Figure 2b. Top: Model A, obtained by increasing the slip contrast between the upper asperity and the background fault region. Bottom: Model B obtained by switching the asperity locations.

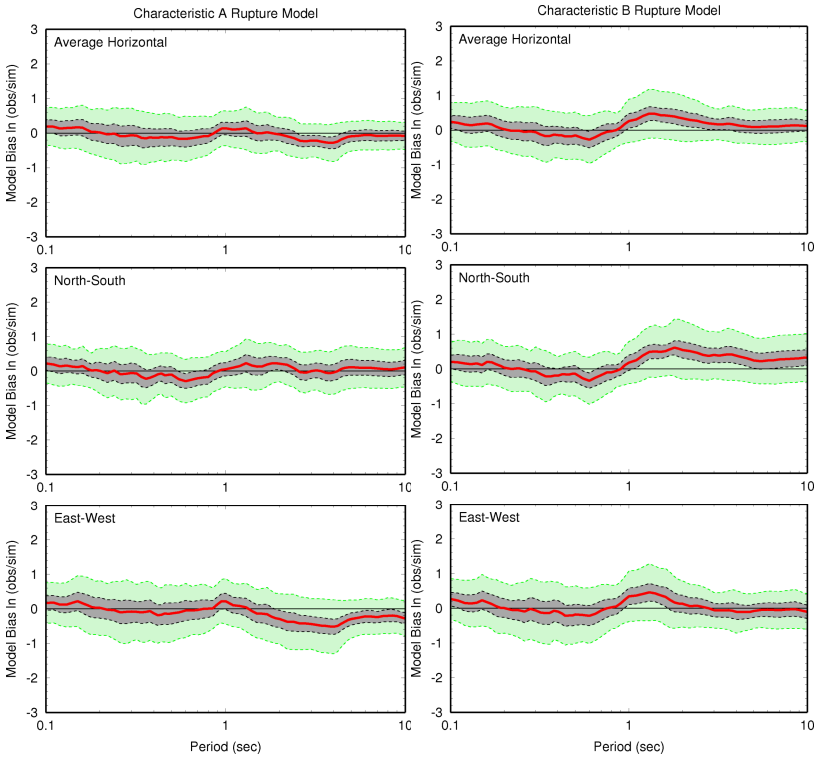

Figure 8. Spectral acceleration goodness-of-fit computed for the average of both horizontal components for the characteristic Models A and B simulations. Red line is mean model bias averaged over 22 sites. Gray shading denotes 90% confidence interval of the mean and green shading denotes interval of one standard deviation.